Serb. Astron. J. № 191 (2015), 59 - 66 **UDC 521.933**
DOI: 10.2298/SAJ1591059V Original scientific paper

EARTH ORIENTATION AND ITS EXCITATIONS BY ATMOSPHERE, OCEANS, AND GEOMAGNETIC JERKS

J. Vondrák and C. Ron

Astronomical Institute, Czech Academy of Sciences, Boční II, 141 00 Prague, Czech Republic

E–mail: *vondrak@ig.cas.cz, ron@asu.cas.cz*

(Received: August 14, 2015; Accepted: September 24, 2015)

SUMMARY: In addition to torques exerted by the Moon, Sun, and planets, changes of the Earth orientation parameters (EOP) are known to be caused also by excitations by the atmosphere and oceans. Recently appeared studies, hinting that geomagnetic jerks (GMJ, rapid changes of geomagnetic field) might be associated with sudden changes of phase and amplitude of EOP (Holme and de Viron 2005, 2013, Gibert and Le Mouël 2008, Malkin 2013). We (Ron et al. 2015) used additional excitations applied at the epochs of GMJ to derive its influence on motion of the spin axis of the Earth in space (precession-nutation). We demonstrated that this effect, if combined with the influence of the atmosphere and oceans, improves substantially the agreement with celestial pole offsets observed by Very Long-Baseline Interferometry. Here we concentrate our efforts to study possible influence of GMJ on temporal changes of all five Earth orientation parameters defining the complete Earth orientation in space. Numerical integration of Brzeziński's broad-band Liouville equations (Brzeziński 1994) with atmospheric and oceanic excitations, combined with expected GMJ effects, is used to derive EOP and compare them with their observed values. We demonstrate that the agreement between all five Earth orientation parameters integrated by this method and those observed by space geodesy is improved substantially if the influence of additional excitations at GMJ epochs is added to excitations by the atmosphere and oceans.

Key words. Earth – reference systems – time

1. INTRODUCTION

Earth orientation parameters (EOP) define the orientation of the Earth in space and, therefore, are important for transformations between terrestrial and celestial reference frames. There are five of them – two components of polar motion (position of spin axis within the Earth), two components of precession-nutation (position of spin axis in space), and proper rotation (measured as Universal Time UT1, or its negatively taken first time derivative, length-of-day) – see Fig. 1. They are regularly monitored by the International Earth Rotation and Reference Systems Service (IERS) established by the IAU and IUGG in 1987. Precession-nutation is dominantly caused by torques exerted by the Moon, Sun, and planets on the rotating flattened Earth, and is now described with extremely high accuracy by the IAU models of nutation (IAU2000) based on rigid-Earth model by Souchay et al. (1999) and applying the non-rigid Earth response by Mathews et al. (2002), and precession (IAU2006) by Capitaine et al. (2003) and Capitaine and Wallace (2006); therefore, only small deviations from these models (celestial pole offsets) are derived from observations.

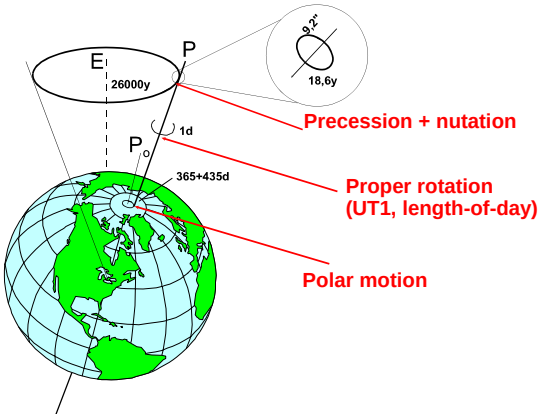

Fig. 1. *Earth Orientation Parameters.*

It was demonstrated earlier by many authors (see, e.g., Barnes et al. 1983, Brzeziński 1994, Gross 2005) that excitations by geophysical fluids (atmosphere, oceans) play dominant role in polar motion and rotational velocity of the Earth. Some effects (about two magnitudes smaller) can also be seen in nutation. However, excitations by geophysical fluids alone cannot fully explain all observed variations of Earth Orientation Parameters (EOP). It was recently noticed that sudden jumps of phase and/or amplitude of all EOP are somehow correlated with geomagnetic jerks (GMJ):

- length-of-day (Holme and de Viron 2005, 2013);
- polar motion (Gibert and Le Mouël 2008);
- nutation (Malkin 2013).

GMJ are rapid changes of the second time derivative of geomagnetic field lasting typically from several months to a year (see Mandea et al. 2010). They are often not detected globally at the same time and their duration is difficult to be determined precisely (Chulliat and Maus 2014). Here we use a simplified assumption that their duration is the same in all cases, and use its value by minimizing the fit to the observed EOP.

We discuss these possibilities in the present study, using the numerical integration of the excitations by geophysical fluids in combination with additional excitations due to GMJ, and comparing the results with the observed values of EOP. To study excitations of polar motion, many authors prefer using the so called geodetic excitations (computed from the observed polar motion) and comparing them with excitations by geophysical fluids. This approach is much easier if compared with the integration approach since it does not require complicated and time consuming looking for optimal initial conditions. However, here we decided to use the integration, mainly for two reasons:

a) Geodetic excitations are computed for the model containing only one (Chandler) resonant frequency. Nevertheless, it would become extremely difficult (and maybe even impossible) to compute them exactly for the more realistic model with two resonant frequencies (Chandler and free core nutation), as is the case of Brzeziński's broad-band Liouville equations that we are using here (see Section).

b) While geodetic excitations are excellent tools to study forced motion, they are less sensitive to the free Chandlerian term - it disappears in geodetic excitations. Thus, it is practically impossible to study changes of its amplitude and phase, which is our main subject of interest in this paper; the expected influence of GMJ is a quasi-instantaneous change of amplitude and phase of only the free part of the motion while its forced periodic part remains unchanged. The tests that we made with geodetic excitations show that their differences from atmospheric and oceanic excitations are rather noisy (their peak values reaching almost 100 mas), so that the episodic additional excitations due to GMJ of comparable amplitudes are invisible.

2. INPUT DATA

We use the following data, covering the interval 1989.00–2014.25:

• *For polar motion and length-of-day changes:* The C04 solution provided by the International Earth Rotation and Reference Systems Service (IERS) at equidistant daily intervals – see Figs. 2 and 3. The latter figure depicts also a long-periodic part due to tidal friction and decadal variations obtained by filtering original data so that only the periods longer than 7 years are retained.

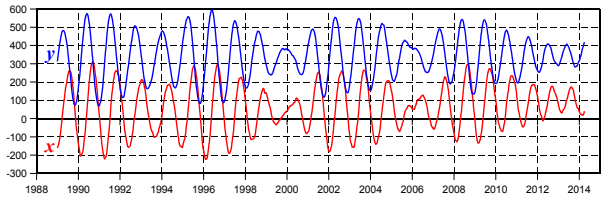

Fig. 2. *Polar motion after IERS C04* [*mas*].

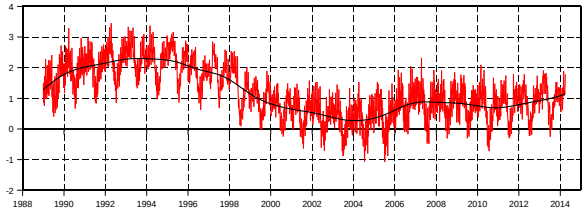

Fig. 3. *Length-of-day changes after IERS C04* [*ms*].

• *For nutation:* VLBI-based observations of celestial pole offsets (differences from the most recent adopted IAU2000/2006 model of precession-nutation) dX, dY: combined solution `ivs14q1X.eops`, provided by the International VLBI Service for Geodesy and Astrometry (IVS). The data

are spaced unevenly in intervals from 1 to 7 days (see Fig. 4). Before using data for comparison with the integrated excited values (see below), the outliers (larger than 1 mas) are removed, the series is filtered (Vondrák 1977) to contain only periods between 60 and 6000 days, and interpolated to 10-day intervals. We also removed the so called Sun-synchronous correction with annual period applied by Mathews et al. (2002) to account for the missing atmospheric effects in their nutation model.

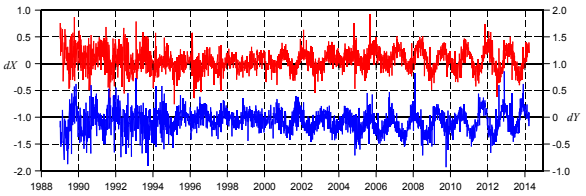

Fig. 4. *Celestial pole offsets after IVS* [*mas*].

• *For atmospheric and oceanic excitations:* effective angular momentum functions $\chi_{1,2,3}$ (defined by Barnes et al. 1983), available at 6-hour intervals from the U.S. National Centers for Environmental Predictions / National Center for Atmospheric Research (NCEP/NCAR) reanalysis (Zhou et al. 2006). Wind plus pressure terms both without and with the Inverted Barometer (IB) correction are used. The former represents an Earth model with 'frozen' oceans, the latter representing a simple oceanic model, in which the oceans react immediately and inversely to pressure changes – see Figs. 5 and 6. It is evident that the IB correction significantly diminishes variations of pressure term. Oceanic excitations used here are those given by the ECCO model (Gross et al. 2005, Gross 2009), computed at 1-day intervals since 1993.0 – see Fig. 7. However, they can be used only for studying polar motions and length-of-day changes since they lack retrograde quasi-diurnal signal (which becomes long-periodic in celestial frame), capable of exciting nutation.

There exist more series of atmospheric/oceanic excitations (e.g., European models ERA and OMCT). We demonstrated earlier (Vondrák and Ron 2014) that they yield systematically larger amplitudes, if compared with NCEP/NCAR and the observed values of celestial pole offsets. This is in agreement with the findings by Brzeziński et al. (2014). Therefore, we concentrate here on NCEP/NCAR and ECCO solutions only.

• *For geomagnetic jerks:* the epochs 1991.0, 1994.0, 1999.0 and 2007.5 given by Malkin (2013), two close epochs 2003.5 and 2004.7 after Olsen and Mandea (2008) and Mandea et al. (2010), and 2011.0 by Chulliat and Maus (2014) are fixed, schematic excitations (see below) with amplitudes estimated from the best fit to observations are used.

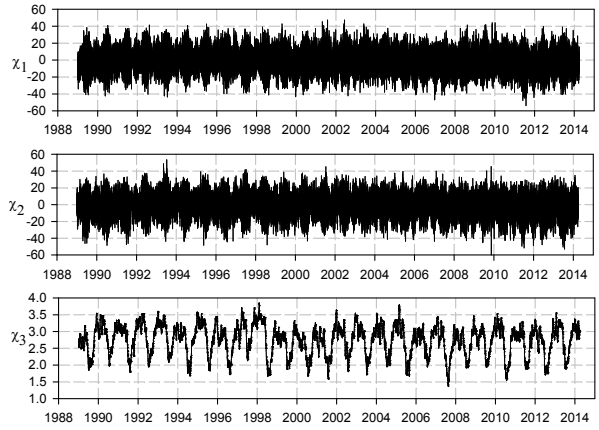

Fig. 5. *NCEP atmospheric angular momentum functions* [10^{-8}] – *wind terms.*

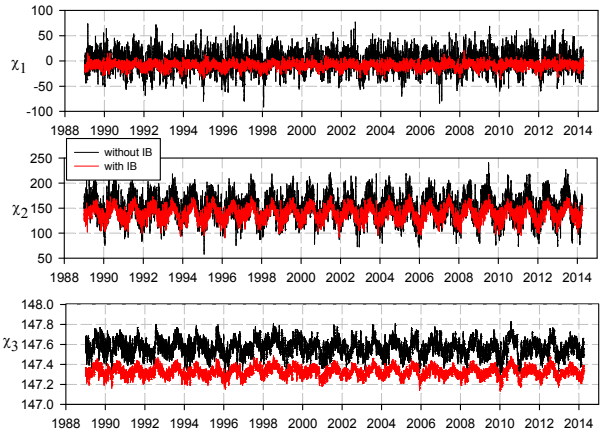

Fig. 6. *NCEP atmospheric angular momentum functions* [10^{-8}] – *pressure terms.*

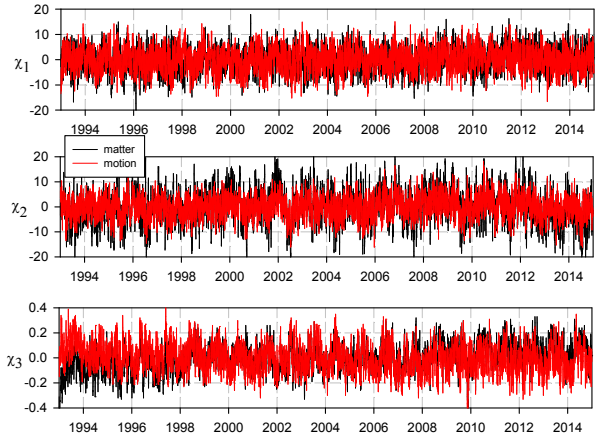

Fig. 7. *ECCO oceanic angular momentum functions* [10^{-8}] – *matter and motion terms.*

3. BROAD-BAND LIOUVILLE EQUATIONS AND THEIR NUMERICAL INTEGRATION

Polar motion and celestial pole offsets excited by geophysical fluids can be derived from numerical integration of Brzeziński's broad-band Liouville equations (Brzeziński 1994) using atmospheric and oceanic angular momentum functions. They are written (in complex form, with $\mathrm{i} = \sqrt{-1}$) as follows: For polar motion, $p = x - \mathrm{i}y$, they read:

$$\begin{aligned}&\ddot{p} - \mathrm{i}(\sigma_\mathrm{C} + \sigma_\mathrm{f})\dot{p} - \sigma_\mathrm{C}\sigma_\mathrm{f} p = \\ &-\sigma_\mathrm{C}\left\{\sigma_\mathrm{f}(\chi_p + \chi_\mathrm{w}) + \sigma_\mathrm{C}(a_p\chi_p + a_\mathrm{w}\chi_\mathrm{w})\right. \\ &\left. + \mathrm{i}\left[(1+a_p)\dot{\chi}_p + (1+a_\mathrm{w})\dot{\chi}_\mathrm{w}\right]\right\}, \end{aligned} \tag{1}$$

for celestial pole offsets, $P = \mathrm{d}X + \mathrm{i}\mathrm{d}Y \approx \Delta\psi \sin\epsilon_0 + \mathrm{i}\Delta\epsilon$ ($\Delta\psi$, $\Delta\epsilon$ being the nutation offsets in longitude and obliquity, respectively), the equations have formally a very similar form:

$$\begin{aligned}&\ddot{P} - \mathrm{i}(\sigma'_\mathrm{C} + \sigma'_\mathrm{f})\dot{P} - \sigma'_\mathrm{C}\sigma'_\mathrm{f} P = \\ &-\sigma_\mathrm{C}\left\{\sigma'_\mathrm{f}(\chi'_p + \chi'_\mathrm{w}) + \sigma'_\mathrm{C}(a_p\chi'_p + a_\mathrm{w}\chi'_\mathrm{w})\right. \\ &\left. + \mathrm{i}\left[(1+a_p)\dot{\chi}'_p + (1+a_\mathrm{w})\dot{\chi}'_\mathrm{w}\right]\right\}. \end{aligned} \tag{2}$$

In Eqs. (1) and (2), σ_C, σ_f are the two main resonance frequencies – Chandler and retrograde free core nutation (RFCN) in the terrestrial frame, σ'_C, σ'_f are the same frequencies expressed in the celestial frame, $\chi_p = \chi_{1p} + \mathrm{i}\chi_{2p}$, $\chi_\mathrm{w} = \chi_{1\mathrm{w}} + \mathrm{i}\chi_{2\mathrm{w}}$ are the effective angular momentum functions (pressure and wind terms, respectively) in the terrestrial frame, χ'_p, χ'_w the same in the celestial frame. Unlike in our preceding studies, here we use more recent values of numerical constants (Koot and de Viron 2011) $a_p = 9.200\times10^{-2}$, $a_\mathrm{w} = 2.628\times10^{-4}$, expressing different reaction on pressure/wind terms.

There is a simple relation between frequency in the terrestrial and celestial reference frames, $\sigma' = \sigma + \Omega$, where $\Omega = 6.30038$ rad/day is the mean speed of rotation of the Earth. Here we use two complex free frequencies $\sigma_\mathrm{f} = -6.31498 + 0.000153\mathrm{i}$, $\sigma_\mathrm{C} = 0.014602 + 0.000083\mathrm{i}$, based on values given by Mathews et al. (2002) in Tab. 3a and Appendix D, respectively. They correspond to periods and quality factors $T_\mathrm{f} = -430.35$d, $Q_\mathrm{f} = 20000$ (in the celestial frame) and $T_\mathrm{C} = 430.30$d, $Q_\mathrm{C} = 88.4$ (in the terrestrial frame). Any complex effective angular momentum function χ in the terrestrial frame can be transformed into χ' in the celestial frame, using a simple formula $\chi' = -\chi\mathrm{e}^{\mathrm{i}\phi}$, where ϕ is the Greenwich sidereal time. Thus, the retrograde quasi-diurnal signal in terrestrial frame appears as a long-periodic signal in the celestial frame.

To integrate Eqs. (1) and (2) numerically, we are using the fourth-order Runge-Kutta method (Press et al. 1992) with 6-hour steps. To this end, we re-wrote the subroutine `rk4` in a complex form. We also introduced substitutions $y_1 = p$, $y_2 = \dot{p} - \mathrm{i}\sigma_\mathrm{f} p$ in Eq. (1) and $Y_1 = P$, $Y_2 = \dot{P} - \mathrm{i}\sigma'_\mathrm{C} P$ in Eq. (2) to get the systems of two first-order complex differential equations instead of one second-order equation. For polar motion they read

$$\begin{aligned}\dot{y}_1 &= \mathrm{i}\sigma_\mathrm{f} y_1 + y_2 \\ \dot{y}_2 &= \mathrm{i}\sigma_\mathrm{C} y_2 - \sigma_\mathrm{C}\left\{\sigma_\mathrm{f}(\chi_p + \chi_\mathrm{w}) + \sigma_\mathrm{C}(a_p\chi_p + a_\mathrm{w}\chi_\mathrm{w})\right. \\ &\left. + \mathrm{i}\left[(1+a_p)\dot{\chi}_p + (1+a_w)\dot{\chi}_w\right]\right\}, \end{aligned} \tag{3}$$

and for celestial pole offsets:

$$\begin{aligned}\dot{Y}_1 &= \mathrm{i}\sigma'_\mathrm{C} Y_1 + Y_2 \\ \dot{Y}_2 &= \mathrm{i}\sigma'_\mathrm{f} Y_2 - \sigma_\mathrm{C}\left\{\sigma'_\mathrm{f}(\chi'_p + \chi'_\mathrm{w}) + \sigma'_\mathrm{C}(a_p\chi'_p + a_\mathrm{w}\chi'_\mathrm{w})\right. \\ &\left. + \mathrm{i}\left[(1+a_p)\dot{\chi}'_p + (1+a_\mathrm{w})\dot{\chi}'_\mathrm{w}\right]\right\}. \end{aligned} \tag{4}$$

We choose the initial values $y_1(0) = p(0)$ and $y_2(0) = \mathrm{i}(\sigma_\mathrm{C} - \sigma_\mathrm{f})p(0)$ for polar motion, $Y_1(0) = P(0)$ and $Y_2(0) = \mathrm{i}(\sigma'_\mathrm{f} - \sigma'_\mathrm{C})P(0)$ for celestial pole offsets, which assures that the quasi-diurnal free motions (both in terrestrial and celestial reference frame) disappear. Integrations are repeated with different values $p(0)$, $P(0)$ to find the best rms fit to observations. It is necessary to stress that the choice of the initial pole position affects only the amplitude and phase of free motions; the forced motions remain intact by the choice.

4. GEOMAGNETIC JERKS AND THEIR SIMULATED EXCITATIONS

In our recent paper (Vondrák and Ron 2014) devoted to celestial pole offsets only, we accounted for the effect of GMJ by simply interrupting numerical integration at GMJ epochs and starting it again with slightly different initial conditions (which is equivalent to delta-shaped excitation). This led to discontinuities of pole position at these epochs, which is physically not acceptable. Thus, we decided to use a 'schematic' excitation function, in the sense introduced by Lambeck (1980, chap. 4.3), capable of changing only the phase and amplitude of the free term during a relatively short time interval without changing neither the mean pole position nor the forced quasi-periodic component of its motion. Consequently, we used additional excitations of a 'double ramp' (or triangular) shape, 200 days (i.e., comparable to the typical length of GMJ) long. This was chosen to obtain continuous pole motion with rapidly changed phase and amplitude of the free term, and its mean position unchanged. The amplitudes of these excitations were estimated to get the best fit with the observations. In order to find how the fit changes with changing the epochs of introducing additional excitations, we shifted the epochs in the interval ±100 days around GMJ epochs. The best fit, in the sense of minimizing the RMS, was obtained when these excitations were centered at GMJ epochs (Ron et al. 2015).

Now we are changing this approach again, in order to use not only the continuous, but also smooth form of the additional excitation. Our choice is a 'cosine', or a bell-like shape, with properties very similar to the preceding one:

$$\frac{a}{2}\left[1+\cos\frac{2\pi(t-t_0)}{\Delta}\right], \qquad (5)$$

where a is the complex amplitude estimated to obtain the best fit to observations, t_0 the GMJ epoch, and Δ is the width of the interval in which the excitation is applied. The tests that we made showed that the optimal width is $\Delta = 200$ days. However, the choice of this value is not very critical – it only determines how fast is the change of phase/amplitude of the resulting motion. The excitation function and its simulated influence on the pole position are displayed in Fig. 8. We also made tests with shifting the epochs of additional excitations by ±180 days from GMJ for polar motion and found that the best agreement is again achieved if GMJ epochs are used. This approach is strictly followed in case of polar motion and celestial pole offsets, length-of-day changes are treated slightly differently (see below). It is necessary to say that the three shapes of additional schematic excitations mentioned above (i.e., delta, triangle, and bell) lead to very similar results; we prefer the last one only because it yields continuous and smooth motion of the pole both in the terrestrial and celestial frame.

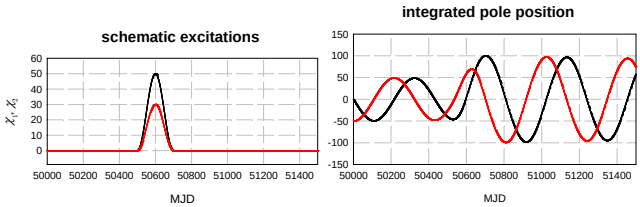

Fig. 8. *Schematic 'bell-shaped' excitation and its simulated effect in pole position.*

5. RESULTS

The integrations were done in two versions: with only atmospheric and oceanic excitations, and with additional excitations due to GMJ added. We always used pressure term without IB correction in combination with oceanic excitation, and the one with IB correction, assuming that the IB correction represents a simple oceanic model.

The amplitudes of additional excitations due to GMJ, which were estimated to provide the best fit to observed values of all Earth orientation parameters, are displayed in Tabs. 1 (polar motion and celestial pole offsets) and 2 (length-of-day changes).

5.1. Polar motion

Since the very long-periodic and secular polar motion is not caused by atmospheric/oceanic effects (these are usually ascribed to the post-glacial rebound – e.g., Vermeersen et al. (1997) or Mitrovica and Milne (1988)), and since we are not interested in very short periods, we used the filter after Vondrák (1977) to remove all periods shorter than 10 and longer than 6000 days from IERS C04 solution (see Section 2) to be directly comparable with the integrated values. We also made some changes in atmospheric excitations, before the integration was made: mean values from both χ_1 and χ_2 were subtracted, the data were smoothed to contain only periods longer than 10 days, and time derivatives needed to integrate Eqs. (1) were computed. The results of integration are graphically demonstrated in Figs. 9 and 10. In both cases, much better agreement with observations is achieved if GMJ excitations are added to atmospheric/oceanic excitations (compare top and bottom plots in both figures). Both rms fit and correlation improved significantly, and the best fit is obtained if NCEP + ECCO excitations are used with GMJ effects (bottom of Fig. 10).

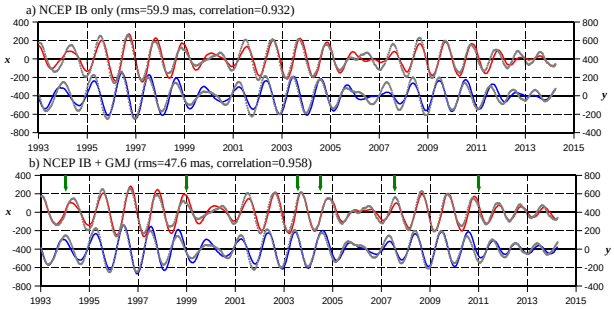

Fig. 9. *Polar motion [mas] – integrated with AAM excitations (full line) and observed (dotted line). Arrows denote the GMJ epochs.*

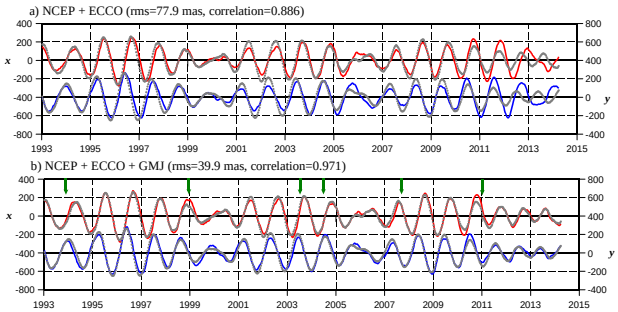

Fig. 10. *Polar motion [mas] – integrated with AAM + OAM excitations (full line) and observed (dotted line). Arrows denote the GMJ epochs.*

Table 1. Amplitudes of additional excitations of polar motion and celestial pole offsets due to GMJ.

	NCEP IB		NCEP+ECCO		NCEP IB	
GMJ epoch	χ_1 [mas]	χ_2 [mas]	χ_1 [mas]	χ_2 [mas]	χ'_1 [mas]	χ'_2 [mas]
1991.0					–0.45	0.40
1994.0	–30	40	5	60	–0.35	1.05
1999.0	25	-5	60	5	–0.60	0.85
2003.5	–35	55	–40	50	0.70	–1.20
2004.7	20	–95	–30	–70	0.25	–0.70
2007.5	–35	0	–35	60	–1.15	–1.45
2011.0	15	–70	110	–65	–0.60	–0.25

Table 2. Amplitudes of additional excitations of length-of-day due to GMJ.

	NCEP IB	NCEP+ECCO
GMJ epoch	$\dot\chi_3$ [μs/day]	$\dot\chi_3$ [μs/day]
1994.0	0.31	0.47
1999.0	–0.08	0.33
2003.5	–0.61	–0.57
2004.7	0.99	0.71
2007.5	0.25	0.14
2011.0	–0.22	–0.23

5.2. Celestial pole offsets

Similarly to polar motion, we removed all periods outside the interval 60–6000 days from CPO given in the IVS solution (Section 2). Atmospheric excitations were converted into celestial frame, the mean values removed, and their time derivatives, needed to integrate Eqs. (2) were calculated. The obtained results are depicted in Fig. 11. Again, from comparison of the top and bottom graph, a significant improvement of the fit to observations is seen when GMJ excitations are added.

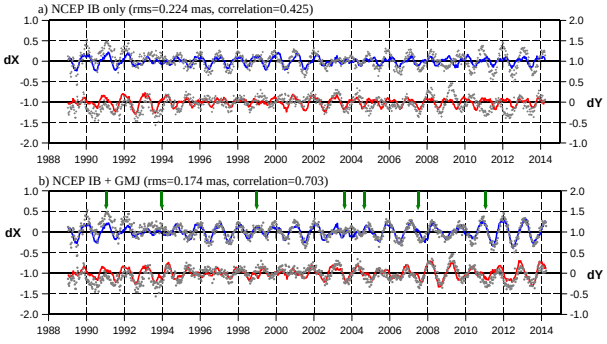

Fig. 11. *Celestial pole offsets [mas] – integrated with AAM (full line) and observed (dotted line). Arrows denote the GMJ epochs.*

5.3. Length-of-day

In the case of length-of-day, the situation differs from the preceding two cases – the relation between length-of-day changes (l.o.d.), expressed in seconds, and excitation is simply (Barnes et al. 1983):

$$\text{l.o.d.} = 86400(\chi_{3\text{w}} + \chi_{3p}) + \text{constant}. \qquad (6)$$

Variations of the Earth's speed of rotation are dominantly caused by tidal effects (deceleration due to the tidal friction and zonal tidal deformations, both caused by the Moon and Sun) and atmospheric/oceanic excitations. There exist also decadal variations of somehow obscure origin, often ascribed to core-mantle coupling. Thus, prior to comparing the observed length-of-day with the excitations, we removed from l.o.d. series: tidal variations as given by IERS Conventions 2010 (Petit and Luzum 2010), and a long-periodic part (due to tidal dissipation and decadal variations) by using a filter by Vondrák (1977) to remove periods longer than 7 years. In addition to atmospheric excitations, we modeled GMJ effects by applying schematic excitations at GMJ epochs defined by Eq. (5). Since the papers by Holme and de Viron (2005, 2013) identify the GMJ epochs with sudden changes of the first derivative of LOD, we applied additional excitations to the time derivative $\dot\chi_3$ and then integrated them to obtain the effect in χ_3. The results for both oceanic models (NCEP IB and NCEP + ECCO) are shown in Figs. 12 and 13, respectively. Similarly to polar mo-

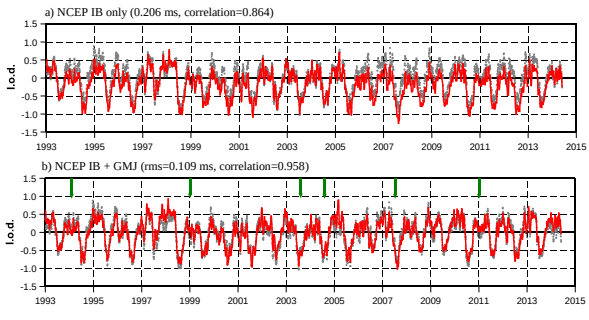

Fig. 12. *Length-of-day changes [ms] – calculated with AAM excitations (full line) and observed (dotted line). Arrows denote the GMJ epochs.*

tion and celestial pole offsets, the significant improvement of the fit due to the inclusion of GMJ effects is evident, but the difference between NCEP IB and NCEP + ECCO is negligible. This is quite natural, since the effect of the oceans is very small if compared with the atmosphere (especially wind effect is dominant) in this case.

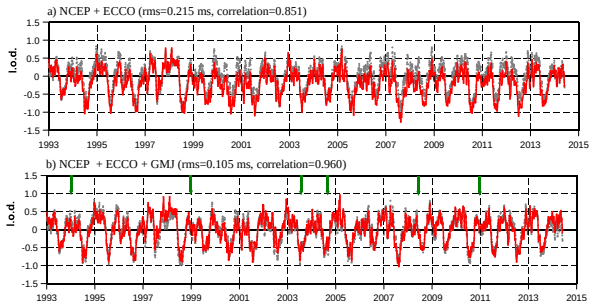

Fig. 13. *Length-of-day changes [ms] – calculated with AAM + OAM excitations (full line) and observed (dotted line). Arrows denote the GMJ epochs.*

6. CONLUSIONS

Geophysical excitations, although dominant in polar motion and speed of rotation, are capable of yielding significant contribution to all Earth orientation parameters. Numerical integration of Brzeziński's broad-band Liouville equations is found to be convenient to account for these effects in polar motion and nutation (represented here as celestial pole offsets) in time domain. However, the comparison of the results based on the excitations by geophysical fluids alone does not provide fully satisfactory results. There still exist relatively rapid changes in all Earth orientation parameters both of the amplitude and phase, unexplained by geophysical fluids. We demonstrate here that additional impulse-like excitations applied at the epochs of GMJ improve the agreement between the excited and observed Earth orientation parameters. The best fit is obtained if NCEP atmospheric plus ECCO oceanic excitations are combined with the effects of geomagnetic jerks, especially in case of polar motion and celestial pole offsets. For the length-of-day changes, the oceanic contribution is only marginal, both NCEP IB and ECCO models yield practically identical results, the inclusion of the GMJ excitation however brigs about significant improvement.

We do not provide here the physical mechanism of how GMJ can influence Earth orientation parameters; we only demonstrate a remarkable coincidence between the two phenomena. Nevertheless, it is well known that geomagnetic coupling between the Earth's mantle and core has a measurable effect. Thus, the probability that GMJ causes the changes of this coupling which, in turn, is reflected in Earth orientation, is very high.

Acknowledgements – This study was made thanks to the grant No. 13-15943S, awarded by the Grant Agency of the Czech Republic.

REFERENCES

Barnes, R. T. H., Hide, R., White, A. A. and Wilson C. A.: 1983, *Proc. R. Soc. Lond.* A, **387**, 31.
Brzeziński, A.: 1994, *Manuscripta geodaetica*, **19**, 157.
Brzeziński, A., Dobslaw, H. and Thomas, M.: 2014, IAG Symp. 139, Springer-Verlag, Berlin Heidelberg, p. 61 (doi: 10.1007/978-3-642-37222-3).
Capitaine, N. and Wallace, P. T.: 2006, *Astron. Astrophys.*, **450**, 855.
Capitaine, N., Wallace, P. T. and Chapront, J.: 2003, *Astron. Astrophys.*, **412**, 567.
Chulliat, A. and Maus, S.: 2014, *J. Geophys. Res. Solid Earth*, **119**, 1531 (doi:10.1003/2013B010604).
Gibert, D. and Le Mouël, J.-L.: 2008, *J. Geophys. Res.*, **113**, B10405.
Gross, R. S., Fukumori, I. and Menemenlis, B.: 2005, *J. Geopys. Res.*, **110**, B09405 (doi:10.1029/2004JB003565).
Gross, R. S.: 2009, *J. Geod.*, **83**, 635 (doi:10.1007/s00190-008-0277-y).
Holme, R. and de Viron, O.: 2005, *Geophys. J. Int.*, **160**, 435.
Holme, R. and de Viron, O.: 2013, *Nature*, **499**, 202.
Koot, L. and de Viron, O.: 2011, *Geophys. J. Int.*, 185, 1255
Lambeck, K.: 1980, The Earth's variable rotation; Geophysical causes and consequences, Cambridge University Press, Cambridge.
Malkin, Z.: 2013, *J. Geodyn.*, **72**, 53.
Mandea, M., Holme, R., Pais, A., Pinheiro, K., Jackson, A. and Verbanac, G.: 2010, *Space Sci. Rev.*, **155**, 147.
Mathews, P. M., Herring, T. A. and Buffet, B. A.: 2002, *J. Geophys. Res.*, **107**, B4, ETG 3 - 1.
Mitrovica, J. X. and Milne, G. A.: 1998, *J. Geopys. Res.*, **103**, 985.
Olsen, N. and Mandea, M.: 2014, *Nature Geosci.*, **1**, 390 (doi:10.1038/ngeo203).
Petit, G. and Luzum, B. (eds.): 2010, IERS Conventions 2010, IERS Tech. Note 36, Ver. Bundesamts für Kartographie und Geodäsie, Frankfurt a. M.
Press, W. H., Teukolsky, S. A., Vetterling, W. T. and Flannery, B. P.: 1992, Numerical Recipes in Fortran 77. The Art of Scientific Computing, 2nd Edition, Cambridge University Press, Cambridge.
Ron, C., Vondrák, J. and Chapanov, Ya.: 2015, in "Proc. IX. Bulgarian-Serbian Astronomical Conference", Publ. Astron. Soc. 'Rudjer Bošković', in press.
Souchay, J., Loysel, B., Kinoshita, H. and Folgueira, M.: 1999, *Astron. Astrophys. Suppl. Series*, **135**, 111.

Vermeersen, L. L., Fournier, A. A. and Sabadini, R.: 1997, *J. Geophys. Res.*, **102**, 27689.
Vondrák, J.: 1977, *Bull. Astron. Inst. Czechosl.*, **28**, 84.
Vondrák, J. and Ron, C.: 2014, *Acta Geodyn. Geomater.*, **11**, 193.
Zhou, Y. H., Salstein, D. A. and Chen, J. L.: 2006, *J. Geophys. Res.*, **111**, D12108 (doi:10.1029/2005JD006608).

УТИЦАЈИ АТМОСФЕРЕ, ОКЕАНА И ГЕОМАГНЕТНОГ ПОЉА НА ПАРАМЕТРЕ ЗЕМЉИНЕ ОРИЈЕНТАЦИЈЕ

J. Vondrák and C. Ron

Astronomical Institute, Czech Academy of Sciences,
Boční II, 141 00 Prague, Czech Republic

E–mail: *vondrak@ig.cas.cz, ron@asu.cas.cz*

УДК 521.933
Оригинални научни рад

Познато је да на промене параметара Земљине оријентације (ЕОП), поред гравитационог дејства Месеца, Сунца и планета, утичу још атмосфера и океани. Резултати неких недавних истраживања указују и на могућу повезаност брзих промена геомагнетног поља (geomagnetic jerks, GMJ) са наглим променама фазе и амплитуде ЕОП-а (Holme and de Viron 2005, 2013, Gibert and Le Mouël 2008, Malkin 2013). Ми смо већ испитивали утицај додатних поремећајних дејстава на померање Земљине осе ротације у простору (прецесија и нутација) током GMJ интервала (Ron et al. 2015). Показали смо да ефекат овог утицаја, уз утицаје атмосфере и океана, знатно побољшава сагласност са посматраним одступањима положаја небеског пола. У овом раду, наше напоре смо усмерили ка испитивању могућег GMJ утицаја на повремене промене свих пет параметара Земљине оријентације. Да бисмо израчунали вредности ЕОП-а и упоредили их са њиховим реализованим вредностима, нумерички смо интегралили широкопојасне Liouville-ове једначине (Brzeziński 1994) које су укључивале утицаје атмосфере и океана, заједно са очекиваним GMJ ефектима. Добијени резултати су потврдили да се сви параметри Земљине оријентације знатно боље усаглашавају са посматрањима, када се ексцитацијама атмосферског и океанског порекла дода и утицај одређених ексцитација у GMJ епохама.